High-order sideband optical properties of a DNA–quantum dot hybrid system [Invited]

Yang Li and Kadi Zhu*

Key Laboratory of Artificial Structures and Quantum Control (Ministry of Education), Department of Physics, Shanghai Jiao Tong University, 800 Dong Chuan Road, Shanghai 200240, China
**Corresponding author: zhukadi@sjtu.edu.cn*

Received February 19, 2013; revised April 9, 2013; accepted April 19, 2013;
posted April 22, 2013 (Doc. ID 185597); published June 11, 2013

High-order sideband nonlinear optical properties in a DNA–quantum dot coupled system are investigated theoretically here. In this paper, we demonstrate the significant enhancement of the third- and fifth-order optical nonlinear properties of the system by applying the pump-probe technique with pump-exciton detuning tuned to zero. It is shown clearly that these phenomena cannot occur without the DNA–quantum dot coupling, implying some potential applications like DNA detection. We can also obtain and tune the significantly amplified sideband beams at frequencies $\omega_p \pm 2\omega_D$. This research could provide people a deeper insight into the nonlinear optical behaviors in coupled DNA–quantum dot systems.

OCIS codes: (190.4710) Optical nonlinearities in organic materials; (270.0270) Quantum optics.
http://dx.doi.org/10.1364/PRJ.1.000016

1. INTRODUCTION

Numerous investigations on high-order nonlinear optical properties, theoretically or experimentally, have been performed. High-order optical nonlinearities in various materials, such as nanoparticles [1–3], InN thin films [4], chalcogenide glasses [5], chalcone and its derivatives [6], BSO and BGO crystals [7], and C_{60}- and C_{70}- toluene solutions [8–10] have been exhibited. Among the wide varieties of materials, biomaterials are some of the most attractive, since they repeatedly present special properties that are not easily detected in inorganic or even organic materials and are usually biodegradable. A type of biomaterial, namely DNA, always appeals to the attention of researchers as an optoelectronic material. With its large dielectric constant and large bandgap [11], a thin film of DNA-cetyltrimethylammonium is utilized in applications as a cladding and host material in nonlinear optical devices, organic light-emitting diodes, and organic field-effect transistors. DNA-based polymers are employed in optically pumped organic solid-state lasers [12]. A more profound comprehension of the high-order nonlinear optical features of DNA will offer more probabilities for new applications. Therefore, voluminous explorations on nonlinear optical properties of DNA materials have been carried out. Samoc *et al.* have considered the nonlinear refractive index and the two-photon absorption coefficient of native (sodium salt) DNA [13]. Krupka *et al.* examined the third-order nonlinear optical properties of thin films of DNA-based complexes with an optical third-harmonic generation technique [14]. Nonlinear optical properties of different materials based on DNA are underway currently.

In this article, we intend to analyze some high-order nonlinear optical properties in a DNA–quantum dot (DNA-QD) coupled system theoretically, which have remained unexplored to date. Since quantum-dot-assisted DNA detection is a promising method for rapid and highly sensitive detection of DNA [15] and even more interesting applications could be exploited, it is important to gain a deeper insight into the high-order nonlinearities of a DNA-QD system. DNA molecules coupled to the peptide quantum dot are driven by pump and probe beams. Several groups have realized a pump-probe technique [16–20], indicating the probability for experimental implementation.

Since metallic quantum dots applied in biological assays are always noxious, the peptide quantum dot, which has no noxiousness to the environment and biological tissues, is a better choice [21,22]. Most recently, the coherent optical spectrum in such a DNA-QD system has been discussed by Li and Zhu [23].

In the present system, the vibration mode of DNA molecules makes such a great contribution that the high-order optical properties could be enhanced significantly. These properties would also be switched by altering the intensity of the pump beam, and the other parameters remain unchanged. In sight of these novel features, we state briefly a potential approach to measure the frequency of the vibration mode of DNA molecules.

2. THEORY

We investigate one of the large amounts of DNA-QDs in an actual reagent, which is displayed in Fig. 1. A strong pump field and a weak probe field act on the DNA-QD system. The Hamiltonian of this system in a rotating frame at ω_p can be expressed as [23]

$$H = \hbar\Delta_p s_z + \sum_{i=1}^{n}\left(\frac{p_i^2}{2m_i} + \frac{1}{2}m_i\omega_i^2 q_i^2\right) - \hbar\Omega_p(s^+ + s^-) + \hbar\vartheta s_z - \mu[E_s s^+ \exp(-i\delta t) + E_s^* s^- \exp(i\delta t)], \quad (1)$$

where s_z, s^+, and s^- describe pseudo-1/2 spin (representing the two-level quantum dot), $\Delta_p = \omega_{eg} - \omega_p$, $\vartheta = \sum_{j=1}^{n}\kappa_j q_j$,

$\Omega_p = \mu E_p/\hbar$ is the Rabi frequency, and $\delta = \omega_s - \omega_c$ is the probe-pump detuning.

Then we can obtain the equations of motion for s_z, s^-, and ϑ via the Heisenberg equation and introduce some damping parameters (Γ_1, Γ_2 and τ_D [24]) just as we usually do. Γ_1 is the exciton relaxation rate, and Γ_2 is the dephasing rate. τ_D is the vibrational lifetime of DNA. According to [25–28], Γ_1 and Γ_2 could be expressed as $\Gamma_1 = \nu_1[1 + 2N(\omega_{eg})]/\hbar$ and $\Gamma_2 = \nu_1[1 + 2N(\omega_{eg})]/2\hbar + 2\nu_2[1 + 2N(0)]/\hbar$, where $\nu_1 = 2\pi D_x(\omega_{eg})$, $\nu_2 = 2\pi D_z(0)$, D_x and D_z are the spectral densities of the respective environments coupled through s_x and s_z to the exciton, and $N(\omega) = 1/[\exp(\hbar\omega/k_BT) - 1]$ is the Boltzman–Einstein distribution of the thermal equilibrium environments. Provided the pure dephasing coupling term is neglected ($\nu_2 = 0$), Γ_1 and Γ_2 have the relation $\Gamma_1 = 2\Gamma_2$, which we adopt in this report. Introducing the corresponding damping and noise terms [29,30], then the equations are as follows:

$$\frac{ds_z}{dt} = -\Gamma_1(s_z + 1/2) + i\Omega_p(s^+ - s^-) + \frac{i\mu E_s \exp(-i\delta t)}{\hbar} s^+ - \frac{i\mu E_s^* \exp(i\delta t)}{\hbar} s^-, \tag{2}$$

$$\frac{ds^-}{dt} = -(i\Delta_p + i\vartheta + \Gamma_2)s^- - 2i\Omega_p s_z - \frac{2i\mu E_s \exp(-i\delta t)}{\hbar} s_z + F_n, \tag{3}$$

$$\frac{d^2\vartheta}{dt^2} + \frac{d\vartheta}{\tau_D dt} + \omega_D^2\vartheta = -\lambda\omega_D^2 s_z + \xi_n, \tag{4}$$

where $\lambda = \sum_{j=1}^{n}(\hbar\kappa_j^2)/(m_j\omega_D^2)$ is the coupling strength of DNA molecules and the quantum dot. In the relatively small volume of aqueous solution here, the longitudinal vibration modes of DNA decay much slower than the other vibration modes [31]. Furthermore, the only longitudinal vibration modes with high frequency should remain since longitudinal vibration modes with low frequency attenuate much more quickly [32]. So, only relatively high-frequency modes should be taken into consideration. We ignore the small difference of ω_i of high-frequency longitudinal modes and replace them with an averaged frequency ω_D for simplification, which should not affect our results. The δ-correlated Langevin noise operator F_n represents the coupling between ϑ and σ_-, the main cause of the decay of vibration mode. F_n has zero mean value $\langle F_n\rangle = 0$ and the correlation relation $\langle F_n(t)F_n^+(t')\rangle \sim \delta(t - t')$. The operator ξ_n stands for the Brownian stochastic force, since the thermal bath of Brownian and non-Markovian processes will affect the vibration mode of DNA molecules [29,33]. The quantum effects on the DNA are only observed in the case $\omega_D\tau_D \gg 1$. The Brownian noise operator can be modeled as Markovian with the decay rate $1/\tau_D$ of the vibration mode. Therefore, the Brownian stochastic force has zero mean value $\langle\xi_n\rangle = 0$ and can be expressed as [33]

$$\langle\xi^+(t)\xi(t')\rangle = \frac{1}{\tau_D\omega_D}\int \frac{\omega + \omega\coth\left(\frac{\hbar\omega}{2k_BT}\right)}{2\pi e^{i\omega(t-t')}}\,d\omega. \tag{5}$$

With the standard methods of quantum optics, the steady-state solutions of Eqs. (2) through (4) read as follows when setting all the time derivatives to zero:

$$s_0 = \frac{2i\Omega_p s_{z0}}{i\lambda s_{z0} - \Gamma_2 - i\Delta_p}, \qquad \vartheta_0 = -\lambda s_{z0}, \tag{6}$$

where s_{z0} is determined by Eq. (7), which is

$$\frac{1}{2}\Gamma_1\Gamma_2^2 + \frac{1}{2}\Gamma_1\Delta_p^2 = (-\Gamma_1\lambda^2)s_{z0}^3 + \left(\frac{-\Gamma_1\lambda^2}{2} + 2\Gamma_1\lambda\Delta_p\right)s_{z0}^2 + (-\Gamma_1\Delta_p^2 - \Gamma_1\Gamma_2^2 + \Gamma_1\lambda\Delta_p - 4\Gamma_2\Omega_p^2)s_{z0}. \tag{7}$$

To extend this formalism beyond weak coupling, we can always rewrite each Heisenberg operator as the sum of its steady-state mean value and a small fluctuation with zero mean value as follows: $s_- = s_0 + \delta s_-$, $s_z = s_{z0} + \delta s_z$, $\vartheta = \vartheta_0 + \delta\vartheta$, which should be substituted into Eqs. (2) through (4). Since the optical drives are weak and classical, we will identify all the operators with their expectation values and omit the quantum and thermal noise terms [16]. Then the linearized Langevin equations can be written as

$$\langle\dot{\delta s}_z\rangle = i\Omega_p(\langle\delta s^{-*}\rangle - \langle\delta s^-\rangle) - \Gamma_1\langle\delta s_z\rangle + \frac{i\mu E_s \exp(-i\delta t)}{\hbar}(s_0^* + \langle\delta s^{-*}\rangle) - \frac{i\mu E_s^* \exp(i\delta t)}{\hbar}(s_0 + \langle\delta s^-\rangle), \tag{8}$$

$$\langle\dot{\delta s}^-\rangle = -(i\Delta_p + \Gamma_2)\langle\delta s^-\rangle - 2i\Omega_p\langle\delta s_z\rangle - i(\vartheta_0\langle\delta s^-\rangle + \langle\delta\vartheta\rangle s_0 + \langle\delta s^-\rangle\langle\delta\vartheta\rangle) - \frac{2i\mu E_s \exp(-i\delta t)}{\hbar}(s_{z0} + \langle\delta s_z\rangle), \tag{9}$$

$$\langle\ddot{\delta\vartheta}\rangle + \frac{\langle\dot{\delta\vartheta}\rangle}{\tau_D} + \omega_D^2\langle\delta\vartheta\rangle = -\lambda\omega_D^2\langle\delta s_z\rangle. \tag{10}$$

With the ansatz $\langle\delta s_z\rangle = s_{z+}\exp(-i\delta t) + s_{z-}\exp(i\delta t) + s_{z+2}\exp(-i2\delta t) + s_{z-2}\exp(i2\delta t)$, $\langle\delta s^-\rangle = s_+\exp(-i\delta t) + s_-\exp(i\delta t) + s_{+2}\exp(-i2\delta t) + s_{-2}\exp(i2\delta t)$, and $\langle\delta\vartheta\rangle = \vartheta_+\exp(-i\delta t) + \vartheta_-\exp(i\delta t) + \vartheta_{+2}\exp(-i2\delta t) + \vartheta_{-2}\exp(i2\delta t)$ [34], all of the equations can then be solved completely. We just list expressions for the higher-order sidebands, with which we are concerned now, as follows:

$$s_{-2} = M_-s_{z-2} + A_-, \tag{11}$$

$$s_{+2} = M_+s_{z+2} + A_+ + M_0s_{z+}E_s, \tag{12}$$

where $M_- = (-2i\Omega_p - is_0M_Q^*)/(\Gamma_2 + i\Delta_p + 2i\delta + i\vartheta_0)$, $M_+ = (-2i\Omega_p - is_0M_Q)/(\Gamma_2 + i\Delta_p - 2i\delta + i\vartheta_0)$, $A_- = -i\vartheta_-s_-/(\Gamma_2 + i\Delta_p + 2i\delta + i\vartheta_0)$, $A_+ = -i\vartheta_+s_+/(\Gamma_2 + i\Delta_p - 2i\delta + i\vartheta_0)$, $M_0 = (-2i\mu)/[\hbar(\Gamma_2 + i\Delta_p - 2i\delta + i\vartheta_0)]$, $M_Q = -\lambda\omega_D^2/(\omega_D^2 - 4\delta^2 - 2i\delta/\tau_D)$, and $s_{z+2} = [i\Omega_p(A_-^* - A_+) - i\Omega_pM_0s_{z+}E_s + i\mu s_-^*E_s/\hbar]/[\Gamma_1 - 2i\delta + i\Omega_p(M_+ - M_-^*)]$. The lower-order terms, that is, $\exp(\pm i\delta t)$ terms, can be obtained with almost the same method.

Finally, we reach to the higher-order nonlinear optical susceptibilities as follows:

$$\chi(\omega_p - 2\omega_s)^{(3)}_{\text{eff}} = \frac{N\mu^2 s_{+2}}{3\varepsilon_0\hbar\Omega_p E_s^2} = \Sigma_3\chi^{(3)}, \tag{13}$$

$$\chi(-3\omega_p + 2\omega_s)^{(5)}_{\text{eff}} = \frac{N\mu^4 s_{-2}}{5\varepsilon_0\hbar^3\Omega_p^3 E_s^{*2}} = \Sigma_5\chi^{(5)}, \tag{14}$$

where N is the number density of DNA-QDs, $\Sigma_3 = (N\mu^4)/(3\varepsilon_0\hbar^3\Gamma_2^3)$ and $\Sigma_5 = (N\mu^6)/(5\varepsilon_0\hbar^5\Gamma_2^5)$.

We can see that the electric displacement can be described by

$$P_{\text{all}} = N\mu\langle\delta s^-\rangle = \varepsilon_0\sum_{j=1}\varepsilon_j E_j = \sum_{j=1}P_j, \tag{15}$$

where j indicates beams with different frequencies. To show the generation of the sideband beams more clearly, we utilize a method similar to [34] to define

$$\frac{-\zeta_3}{100} = \frac{\text{Im}(P_{\omega_p-2\omega_s})\omega_{eg}z}{2c\varepsilon_0|E_s|} = \frac{N\mu\,\text{Im}(s_{+2})\omega_{eg}z}{2c\varepsilon_0|E_s|}, \tag{16}$$

$$\frac{-\zeta_5}{100} = \frac{\text{Im}(P_{-3\omega_p+2\omega_s})\omega_{eg}z}{2c\varepsilon_0|E_s|} = \frac{N\mu\,\text{Im}(s_{-2})\omega_{eg}z}{2c\varepsilon_0|E_s|}, \tag{17}$$

which imply that the third-order and the fifth-order generated sideband are ζ_3% and ζ_5% of the amplitude of the signal beam, respectively. As we know, the imaginary part results from the damping effect, positive for absorption and negative for generation, which is just what the negative sign in the definitions of ζ_3 and ζ_5 refers to. To verify our method, we investigate an input–output amplitude change of a beam propagating through a kind of material whose dielectric constant is ε. The amplitude of output beam should be

$$E_o = E_i\,\exp(-\text{Im}(\varepsilon)\omega z/2c), \tag{18}$$

where E_i, ω, z, and c are input amplitude, frequency of the beam, propagation distance, and light velocity in the vacuum, respectively. Then we have

$$E_o \approx E_i(1 - \text{Im}(\varepsilon)\omega z/2c). \tag{19}$$

Therefore, it is proper to regard $-E_i\,\text{Im}(\varepsilon)\omega z/2c$ as the generated (or absorbed) part. Since the differences of frequencies from exciton frequency ω_{eg} of sideband beams are so small, they can just be presented with ω_{eg} in our case. If $\zeta_3(\zeta_5)$ is positive, it indicates generation, and if $\zeta_3(\zeta_5)$ is negative, it indicates absorption.

3. RESULTS AND DISCUSSIONS

To illustrate the numerical results, we select the realistic DNA-QD system, in which a peptide quantum dot is linked with several DNA molecules as demonstrated in Fig. 1. Although DNA molecules in solution form can be distorted, we can extend these molecules into linear form with electromagnetic field or fluid force [35]. In our theoretical calculation, we choose $\omega_D = 40$ GHz and $\tau_D = 5$ ns as the vibration frequency and lifetime of DNA molecules [36–39]. We can safely pick $\Gamma_1 = 16$ GHz as the decay rate of the peptide quantum dot for

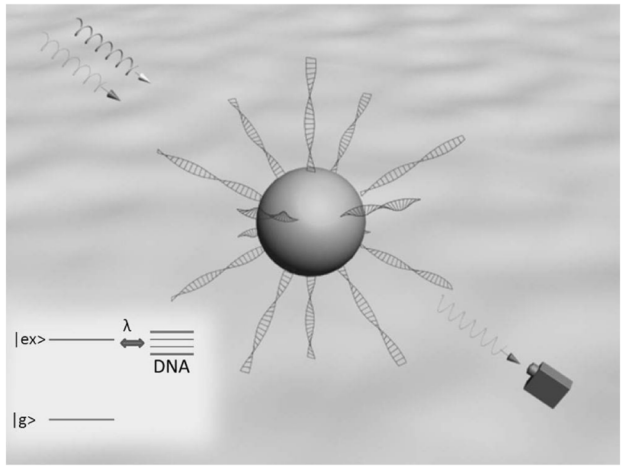

Fig. 1. DNA and peptide quantum dot coupling system: a peptide quantum dot coupled to DNA molecules in the simultaneous presence of two optical fields. The energy level structure of the quantum dot dressed by the vibrational modes of DNA molecules is also shown.

any practical purpose [40]. As to the number density of DNA-QDs N, we can choose $N = 1\times10^{16}$ m^{-3} [41], which is fairly enough to show our results. The exciton frequency is $\omega_{eg} = 2.4\times10^5$ GHz [21] and propagation distance is $z = 0.5$ m. We set the amplitude of the probe beam to be 1% of the pump beam.

Figure 2(a) [2(c)] plots the third-order (fifth-order) optical dispersion $\text{Re}\,\chi^{(3)}$ ($\text{Re}\,\chi^{(5)}$) and third-order (fifth-order) nonlinear absorption $\text{Im}\,\chi^{(3)}$ ($\text{Im}\,\chi^{(5)}$) as functions of probe-exciton detuning $\Delta_s = \omega_s - \omega_{eg}$ with $\Delta_p = 0$ and $\lambda = 0$, while Fig. 2(b) [2(d)] shows the third-order (fifth-order) optical dispersion $\text{Re}\,\chi^{(3)}$ ($\text{Re}\,\chi^{(5)}$) and third-order (fifth-order) nonlinear absorption $\text{Im}\,\chi^{(3)}$ ($\text{Im}\,\chi^{(5)}$) as functions of probe-exciton detuning $\Delta_s = \omega_s - \omega_{eg}$ with $\Delta_p = 0$ but $\lambda = 2$ GHz. This reveals that if we fix the pump beam on-resonance with the exciton and scan through the frequency spectrum, we could obtain large strengthened higher-order optical nonlinear effects at frequencies $\omega_s = \omega_{eg} \pm (\omega_D/2)$ and $\omega_s = \omega_{eg} \pm \omega_D$. This phenomenon stems from the quantum interference between the vibration mode of DNA molecules and the beat of the two optical fields via the exciton when probe-pump detuning δ is adjusted equal to (or half) the frequency of the vibration mode of DNA molecules. If we ignore the coupling, then $\lambda = 0$, and the enhancement of high-order optical features will disappear completely as has been demonstrated in Figs. 2(a) and 2(c). Therefore, the importance of the coupling between the quantum dot and DNA molecules is evident since the enhancement of high-order optical properties could not occur in such a system when $\lambda = 0$. Furthermore, we can propose a scheme to measure the frequency of the vibration mode of DNA molecules by exploiting the phenomenon above. From Figs. 2(b) and 2(d), we can clearly see that as the frequency of the vibration mode is $\omega_D = 40$ GHz, the four sharp peaks appear at ±20 GHz and ±40 GHz, which have certain relations with the mode frequency. This means that if we first adapt the pump beam appropriately and scan the probe frequency across the exciton frequency in the spectrum, we could straightforwardly acquire the accurate vibration frequency of DNA, which suggests some potential future applications. Here is an instance. A sort of DNA molecule that experienced a mutation should have a difference in weight

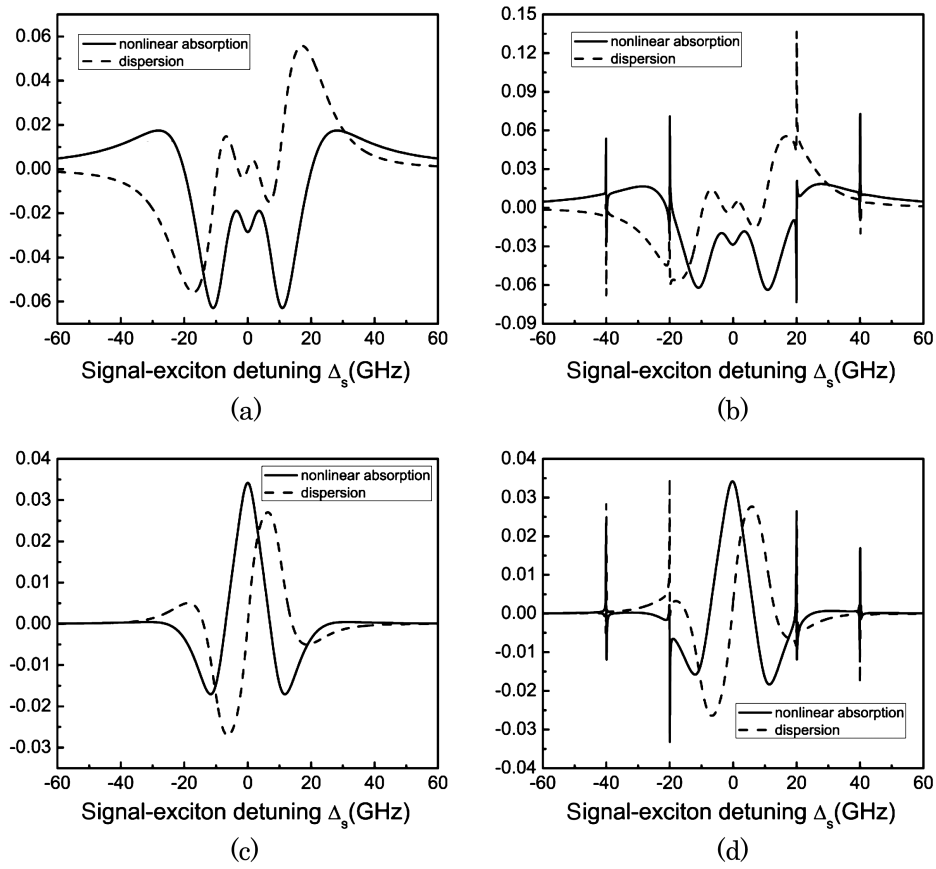

Fig. 2. Optical dispersions and nonlinear absorptions (in units of Σ_3 and Σ_5 for $\chi(\omega_p - 2\omega_s)^{(3)}_{\text{eff}}$ and $\chi(-3\omega_p + 2\omega_s)^{(5)}_{\text{eff}}$, respectively) with pump beam on-resonance ($\Delta_p = 0$). (a) Third-order optical dispersion and nonlinear absorption as functions of probe-exciton detuning Δ_s in the case $\lambda = 0$. (b) Third-order optical dispersion and nonlinear absorption as functions of probe-exciton detuning Δ_s in the case $\lambda = 2$ GHz. (c) Fifth-order optical dispersion and nonlinear absorption as functions of probe-exciton detuning Δ_s in the case $\lambda = 0$. (d) Fifth-order optical dispersion and nonlinear absorption as functions of probe-exciton detuning Δ_s in the case $\lambda = 2$ GHz.

or length from those of original DNA, leading to a shift of the mode frequency of DNA. Then the spectrum should also be modified, that is, the four peaks or dips would drift. Since there exist four peaks and dips and their frequencies are considerably distinguished from those of pump and probe beams, they should be relieved from the disturbance of input beams and could be detected easily. This means small alterations of DNA molecules could be detected. If a normal gene of the DNA turns into a cancer genes giving rise to a shift of the frequency of DNA vibration mode, the mutation will be recognized just by scanning the spectrum.

Figure 3 shows that the ζ_3 value caused by the third-order nonlinearity ($\omega_p - 2\omega_s$ term) varies with δ around two points. We choose $\Omega_p = 5$ GHz as the Rabi frequency of the pump beam. The only different parameter between Figs. 3(a) and 3(b) is exciton-pump detuning Δ_p, that is, $\Delta_p = -\omega_D$ for Fig. 3(a) and $\Delta_p = 1.25\omega_D$ for Fig. 3(b). We see that there are transparent windows near, though not exactly at, the points $\delta = -\omega_D$ and $\delta = \omega_D$ in Figs. 3(a) and 3(b), respectively. The ζ_3 value at $\delta/\omega_D = -1(\delta/\omega_D = 1)$ in Fig. 3(a) [3(b)] is apparently larger than zero, implying that the sideband beam, whose frequency is $\omega_p - 2\omega_D$ ($\omega_p + 2\omega_D$), is amplified. The phenomenon can be understood in the point of view of parametric process, which leaves the quantum state of the material unchanged. As an example, we take the Fig. 3(a) condition into consideration. At the point $\delta/\omega_D = -1$ in Fig. 3(a), we can see that the transitions between the virtual levels [dashed levels in Fig. 3(c)] and the real level [solid level in Fig. 3(c)] lead to the generation of sideband beam $\omega_p - 2\omega_D$. The final quantum state of the system remains the same as the initial, as has been shown in the process. Actually, in a parametric process, population resides in the virtual levels only for a significantly short interval of the order $\hbar/\Delta E$, where ΔE is the difference between the virtual level and the nearest real level. Intervals of those two virtual levels in the middle of the condition we analyze here is relatively large, providing sufficient time to realize the emission. This can also throw light on the dip of Fig. 4(b). The sideband generation (or absorption) effect can also be a potential approach to DNA detection.

The generation of the sideband beam at $\omega_p \pm 2\omega_D$ can be tuned by adjusting the power of the pump beam (or Rabi frequency Ω_p) and exciton-pump detuning Δ_p, as has been shown in Fig. 4, for instance. Figure 4(a) demonstrates the ζ_3 value as a function of Rabi frequency with $\Delta_p = \delta = -\omega_D$, while Fig. 4(b) shows the ζ_3 value as a function of exciton-pump detuning with $\Omega_p = 5$ GHz and $\delta = -\omega_D$. In Fig. 4(a), the $\omega_p - 2\omega_D$ sideband beam is amplified for the most part and reaches its maximum at about 5 GHz. However, there is a suppressive window around 6 GHz. A transparent window appears in Fig. 4(b) near the point $\Delta_p = -\omega_D$, just as what we can see in Fig. 3. A more elaborative observation on Fig. 4(a) is needed. The physics origin of the dip should also be that of the Fano-like asymmetric lineshape. The vibration mode of DNA could be regarded as the supplier of a stack of levels

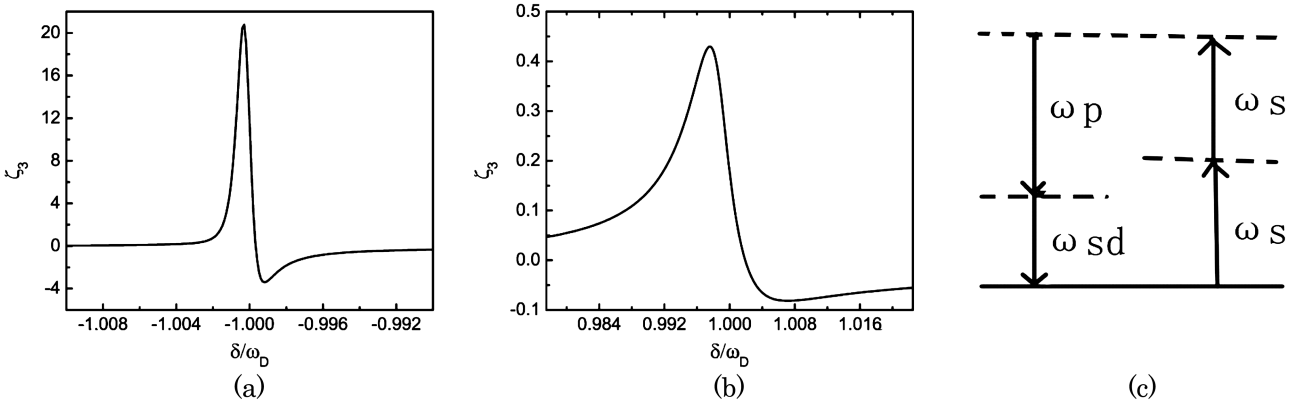

Fig. 3. ζ_3 value caused by third-order nonlinearity with pump beam off-resonance. (a) ζ_3 value as a function of probe-pump detuning in the case $\Delta_p = -\omega_D$. (b) ζ_3 value as a function of probe-pump detuning in the case $\Delta_p = 1.25\omega_D$. (c) Parametric process of point $\delta/\omega_D = -1$ in Fig. 3(a), where $\omega_{\mathrm{sd}} = \omega_p - 2\omega_D$ is the frequency of the sideband beam.

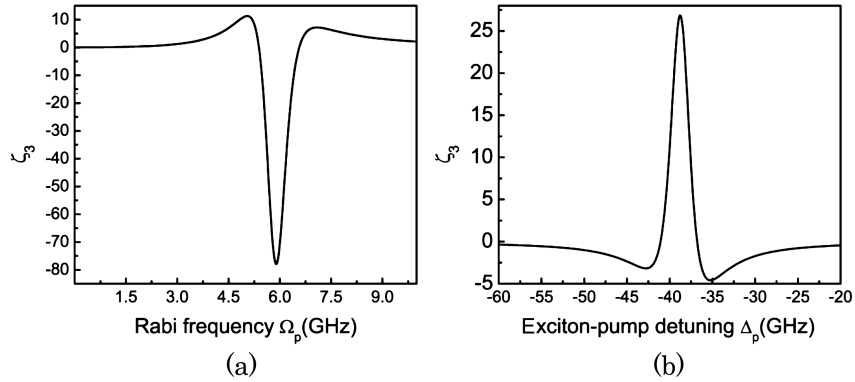

Fig. 4. ζ_3 value by third-order nonlinearity with different Rabi frequency and exciton-pump detuning. (a) ζ_3 value as a function of Rabi frequency in the case $\Delta_p = -\omega_D$ and $\delta = -\omega_D$. (b) ζ_3 value as a function of exciton-pump detuning Δ_p in the case $\delta = -\omega_D$ and $\Omega_p = 5$ GHz.

to the quantum dot (see Fig. 1). This level stack proffers the probability of the quantum interference between the two transition processes (a part of the parametric process), namely the direct transition from $|g\rangle$ to the stack and the indirect transition from $|g\rangle$ through $|e\rangle$ and the coupling to the stack. When the intensity of the pump beam is adjusted properly and a constructive or destructive interference of the two transition paths is realized, a peak or dip should come into being. The Fano-like asymmetric lineshape, which also stems from the quantum interference, is now a natural consequence.

In fact, sideband beams can also come from fifth-order nonlinearity, though much smaller than third-order. We just figure out some main properties as shown in Fig. 5. In Fig. 5(a) [Fig. 5(b)], we choose $\Delta_p = -\omega_D$ and $\delta = -\omega_D$ ($\delta = \omega_D$) as the main parameters to show the ζ_5 value as a function of Rabi frequency. We can see that if the pump beam is weak, sideband beams $\omega_p \pm 2\omega_D$ experience no generation or absorption. Only a transparent window around the Rabi frequency 6 GHz is proper if one expects to get sideband beams. The physics of Fig. 5 should have no more contents than those of Fig. 4(a).

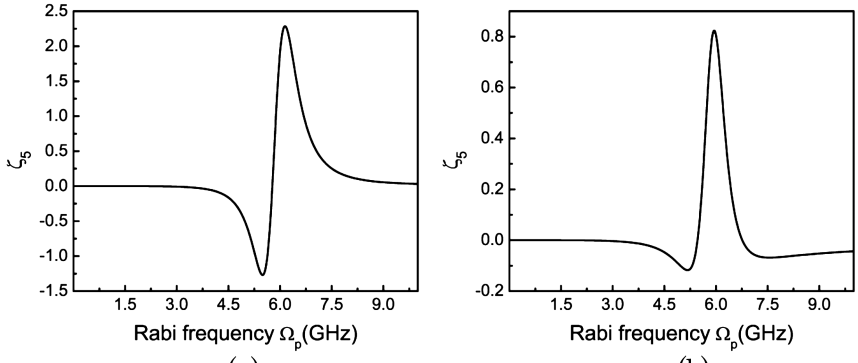

Fig. 5. ζ_5 value caused by fifth-order nonlinearity with exciton-pump detuning $\Delta_p = -\omega_D$ and different δ. (a) ζ_5 value as a function of Rabi frequency in the case $\delta = -\omega_D$. (b) ζ_5 value as a function of Rabi frequency in the case $\delta = \omega_D$.

4. CONCLUSION

In conclusion, we have proposed a theoretical model for a DNA-QD hybrid system in the presence of a strong pump beam and a weak probe beam. The coupling leads to great enhancement of higher-order susceptibilities at four points, namely $\Delta_s = \pm 20$ GHz and $\Delta_s = \pm 40$ GHz, which may be of potential use in frequency measurement. Furthermore, sideband beams at $\omega_p \pm 2\omega_D$ can be generated and tuned by adjusting some parameters properly. We believe that such a phenomenon may lead people to more knowledge of nonlinear optical properties of the coupling quantum dot-DNA system. We hope our results can be checked experimentally in the near future.

ACKNOWLEDGMENTS

This study was supported by the National Natural Science Foundation of China (Nos. 10974133 and 11274230) and the Ministry of Education Program for Ph.D.

REFERENCES

1. E. L. Falcao-Filho, B. de Araujo, and J. J. Rodrigues, "High-order nonlinearities of aqueous colloids containing silver nanoparticles," J. Opt. Soc. Am. B **24**, 2948–2956 (2007).
2. D. Rativa, R. E. de Araujo, and A. S. L. Gomes, "Nonresonant high-order nonlinear optical properties of silver nanoparticles in aqueous solution," Opt. Express **16**, 19244–19252 (2008).
3. R. A. Ganeev, M. Suzuki, M. Baba, M. Ichihara, and H. Kuroda, "Low- and high-order nonlinear optical properties of Au, Pt, Pd, and Ru nanoparticles," J. Appl. Phys. **103**, 063102 (2008).
4. Z. Q. Zhang, W. Q. He, C. M. Gu, W. Z. Shen, H. Ogawa, and Q. X. Guo, "Determination of the third- and fifth-order nonlinear refractive indices in InN thin films," Appl. Phys. Lett. **91**, 221902 (2007).
5. F. Smektala, C. Quemard, V. Couderc, and A. Barthelemy, "Non-linear optical properties of chalcogenide glasses measured by Z-scan," J. Non-Cryst. Solids **274**, 232–237 (2000).
6. B. Gu, W. Ji, X. Q. Huang, P. S. Patil, and S. M. Dharmaprakash, "Nonlinear optical properties of 2,4,5-trimethoxy-4-nitrochalcone: observation of two-photon-induced excited-state nonlinearities," Opt. Express **17**, 1126–1135 (2009).
7. R. A. Ganeev, A. I. Ryasnyanskii, and R. I. Tugushev, "Effect of higher order nonlinear optical processes on optical absorption in the photorefractive BSO and BGO crystals," Opt. Spectrosc. **96**, 526–531 (2004).
8. E. Koudoumas, F. Dong, S. Couris, and S. Leach, "High order nonlinear optical response of fullerene solutions in the nanosecond regime," Opt. Commun. **138**, 301–304 (1997).
9. E. Koudoumas, F. Dong, M. D. Tzatzadaki, S. Couris, and S. Leach, "High-order nonlinear optical response of C_{60}-toluene solutions in the sub-picosecond regime," J. Phys. B **29**, L773–L778 (1996).
10. R. A. Ganeev, G. S. Boltaev, R. I. Tugushev, T. Usmanov, M. Baba, and H. Kuroda, "Low- and high-order nonlinear optical characterization of C_{60}-containing media," Eur. Phys. J. D **64**, 109–114 (2011).
11. S. T. Birendra, S. N. Serdar, and G. G. James, "Bio-organic optoelectronic devices using DNA," Adv. Polym. Sci. **223**, 189–212 (2010).
12. Z. Yu, W. Li, J. A. Hagen, Y. Zhou, D. Klotzkin, J. G. Grote, and A. J. Steckl, "Photoluminescence and lasing from deoxyribonucleic acid (DNA) thin films doped with sulforhodamine," Appl. Opt. **46**, 1507–1513 (2007).
13. M. Samoc, A. Samoc, and J. G. Grote, "Complex nonlinear refractive index of DNA," Chem. Phys. Lett. **431**, 132–134 (2006).
14. O. Krupka, A. E. Ghayoury, I. Rau, B. Sahraoui, J. G. Grote, and F. Kajzar, "NLO properties of functionalized DNA thin films," Thin Solid Films **516**, 8932–8936 (2008).
15. C. Y. Zhang, H. C. Yeh, M. T. Kuroki, and T. H. Wang, "Single-quantum-dot-based DNA nanosensor," Nat. Mater. **4**, 826–831 (2005).
16. S. Weis, R. Rivière, S. Deléglise, E. Gavartin, O. Arcizet, A. Schliesser, and T. J. Kipperberg, "Optomechanically induced transparency," Science **330**, 1520–1523 (2010).
17. J. D. Teufel, D. Li, M. S. Allman, K. Cicak, A. J. Sirois, J. D. Whittaker, and R. W. Simmonds, "Circuit cavity electromechanics in the strong-coupling regime," Nature **471**, 204–208 (2011).
18. A. H. Safavi-Naeini, T. P. M. Alegre, J. Chan, M. Eichenfield, M. Winger, Q. Lin, J. T. Hill, D. E. Chang, and O. Painter, "Electromagnetically induced transparency and slow light with optomechanics," Nature **472**, 69–73 (2011).
19. J. J. Li and K. D. Zhu, "A scheme for measuring vibrational frequency and coupling strength in a coupled annomechancial resonator-quantum DTO system," Appl. Phys. Lett. **94**, 063116 (2009).
20. W. He, J. J. Li, and K. D. Zhu, "Coupling-rate determination based on radiation pressure-induced normal mode splitting in cavity optomechanical systems," Opt. Lett. **35**, 339–341 (2010).
21. N. Amdursky, M. Molotskii, E. Gazit, and G. Rosenman, "Self-assembled bioinspired quantum dots: optical properties," Appl. Phys. Lett. **94**, 261907 (2009).
22. N. Amdursky, M. Molotskii, E. Gazit, and G. Rosenman, "Elementary building blocks of self-assembled peptide nanotubes," J. Am. Chem. Soc. **132**, 15632–15636 (2010).
23. J. J. Li and K. D. Zhu, "Coherent optical spectroscopy in a biological semiconductor quantum dot-DNA hybrid system," Nano. Res. Lett. **7**, 1–7 (2012).
24. C. M. Donega, M. Bode, and A. Meijerink, "Size-and temperature-dependence of exciton lifetimes in CdSe quantum dots," Phys. Rev. B **74**, 085320 (2006).
25. C. W. Gardiner and P. Zoller, *Quantum Noise*, 2nd ed. (Springer, 2000).
26. D. F. Walls and G. J. Milburn, *Quantum Optics* (Springer, 1994).
27. H. Carmichael, *Statistical Methods in Quantum Optics* (Springer, 1999).
28. H. P. Breuer and F. Petruccione, *The Theory of Open Quantum Systems* (Oxford University, 2002).
29. C. W. Gardiner and P. Zoller, "Quantum kinetic theory. V. Quantum kinetic master equation for mutual interaction of condensate and noncondensate," Phy. Rev. A **61**, 033601 (2000).
30. G. J. Milburn, K. Jacobs, and D. F. Walls, "Quantum-limited measurements with the atomic force microscope," Phy. Rev. A **50**, 5256–5263 (1994).
31. B. H. Dorfman, "The effects of viscous water on the normal mode vibrations of DNA," Dissert. Abstr. Int. **45**, 2213 (1984).
32. B. H. Dorfman and L. L. Zandt, "Vibration of DNA polymer in viscous solvent," Biopolymers **22**, 2639–2665 (1983).
33. V. Giovannetti and D. Vitali, "Phase-noise measurement in a cavity with a movable mirror undergoing quantum Brownian motion," Phy. Rev. A **63**, 023812 (2001).
34. H. Xiong, L. G. Si, A. S. Zheng, X. X. Yang, and Y. Wu, "Higher-order sidebands in optomechanically induced transparency," Phys. Rev. A **86**, 013815 (2012).
35. J. F. Marko and E. D. Siggia, "Stretching DNA," Macromolecules **28**, 8759–8770 (1995).
36. G. S. Edwards, C. C. Davis, J. D. Saffer, and M. L. Swicord, "Microwave-field-driven acoustic modes in DNA," Biophys. J. **47**, 799–807 (1985).
37. C. L. Yuan, H. M. Chen, X. W. Lou, and L. A. Archer, "DNA bending stiffness on small length scales," Phys. Rev. Lett. **100**, 018102 (2008).
38. R. Gill, I. Willner, I. Shweky, and U. Banin, "Fluorescence resonance energy transfer in CdSe/ZnS-DNA conjugates: probing hybridization and DNA cleavage," J. Phys. Chem. B **109**, 23715–23719 (2005).
39. B. K. Adai, "Vibrational resonances in biological systems at microwave," Biophys. J. **82**, 1147–1152 (2002).
40. M. J. Tsay, M. Trzoss, L. X. Shi, X. X. Kong, M. Selke, E. M. Jung, and S. Weiss, "Singlet oxygen production by peptide-coated quantum dot-photosensitizer conjugates," J. Am. Chem. Soc. **129**, 6865–6871 (2007).
41. Y. H. Chen, L. Wang, and W. Jiang, "Micrococcal nuclease detection based on peptide-bridged energy transfer between quantum dots and dye-labeled DNA," Talanta **97**, 533–538 (2012).